J Appl Electrochem (2009) 39:1045–1051
DOI 10.1007/s10800-008-9756-3

ORIGINAL PAPER

Influence of ethylene glycol, ethanol and formic acid on platinum and ruthenium electrodeposition on carbon support material

Juan Manuel Sieben · Marta M. E. Duarte · Carlos E. Mayer · Julio C. Bazán

Received: 3 July 2008 / Accepted: 10 December 2008 / Published online: 23 December 2008

Abstract Carbon supported Pt–Ru catalysts were prepared by potentiostatic deposition at −0.5 V from $H_2PtCl_6 + RuCl_3$ in H_2SO_4 solution in the presence of ethylene glycol (EG), ethanol (EtOH) and formic acid (HCOOH) as stabilizing agents. The active surface area of the Pt–Ru catalyst was determined by Cu-UPD. The highest value was obtained with HCOOH added, followed by EtOH, and EG. SEM and AFM images showed that the mean particle size of the Pt–Ru nanoparticles was three or four times smaller in the presence of a stabilizer. Electrocatalytic activity measurements indicated that the most active electrode for methanol electrooxidation was obtained with EtOH as additive, followed by EG. The electrode prepared with HCOOH additive gave lower catalytic activity than that without stabilizing agent.

Keywords Pt–Ru nanostructured catalyst · Electrodeposition · Ethylene glycol · Ethanol · Formic acid · Methanol oxidation

J. M. Sieben (✉) · M. M. E. Duarte · C. E. Mayer
Instituto de Ingeniería Electroquímica y Corrosión (INIEC), Bahía Blanca, Argentina
e-mail: jmsieben@uns.edu.ar

M. M. E. Duarte · C. E. Mayer · J. C. Bazán
Comisión de Investigaciones Científicas de la Provincia de Buenos Aires (CIC), Buenos Aires, Argentina

J. C. Bazán
Departamento de Química, Universidad Nacional del Sur. Av. Alem 1253, 8000 Bahía Blanca, Argentina

1 Introduction

The preparation of nanostructured catalyst over carbonaceous support materials by electrochemical procedures in aqueous solution has received considerable recent attention. These techniques offer some control over the catalyst physico-chemical properties because: (a) they allow variation of the particle size and (b) they offer an effective way to deposit platinum and other noble metal catalysts selectively at desired locations in the electrode with both ionic and electronic access [1]. Electrodeposition by pulse current [2–4], direct current [5], constant potential or consecutive potential steps [6–15] and cyclic voltammetry [16, 17], have been used to deposit platinum and Pt–Ru bimetallic catalysts onto carbon substrates.

The production of catalyst nanoparticles by electrochemical techniques is advantageous, because the crucial steps in nanoparticle formation can be controlled by the selection of current density or overpotential (physical control), and the use of complexing agents and grain refiners (chemical control) [18, 19]. The current density or the overpotential is responsible for the number and size of nuclei. The use of organic additives facilitates control of the crystallization process. In addition, surface activation of the carbon support by electrochemical oxidation produces surface groups that act as attachment centers for metallic particles.

Stabilizing agents are used to prevent the agglomeration of nano-sized catalyst metals, e.g. polyvinyl pyrolidine interacts with Pt–Ru catalyst surface sites [20], EDTA, tartaric acid and citric acid have been used as growth inhibitors in silver, copper, zinc, nickel and tin electrodeposition [21–25]. Similar effects are observed in the chemical reduction of Pt and Pt–Ru in aqueous solution containing one or more alcoholic components, especially

ethylene glycol (EG) as reducing agent [26–28]. Additionally, EG addition can prevent particle agglomeration [29]. When a reducing compound as EG is present two different deposition processes, electrophoretic deposition and electrodeposition, may compete in the catalyst deposit formation. The basic difference between the electrophoretic deposition process (EPD) and the electrodeposition process (ED) is that the former is based on the transport and deposition of colloidal particles suspended in a solvent whereas the later is based on the transport and reduction of ionic species. The catalysts prepared under these conditions are expected to present a different behavior than those prepared only by electrodeposition without stabilizer.

In this work, supported Pt–Ru nanostructured catalysts are prepared by electrodeposition in the presence of different organic molecules used as stabilizers. The effect of ethylene glycol (EG), ethanol (EtOH) and formic acid (HCOOH) on the particle size and the active surface area is discussed. The activity of these electrodes in the methanol oxidation reaction was evaluated.

2 Experimental

Glassy carbon (GC) discs and graphite cloths (GC-10) of 0.07 and 1 cm^2 geometric area, respectively, were used as catalyst support. Previously to Pt–Ru electrodeposition, the GC electrodes were polished with emery paper (grit 1200) and alumina of grade 1 and 0.3 μm. The GC-10 electrodes were cleaned with acetone before use; afterward they were dried and impregnated with $H_2PtCl_6 + RuCl_3$ solution for 15 min.

Electrochemical measurements were carried out in a conventional glass cell at room temperature. The counterelectrode was a platinum sheet, separated from the working electrode compartment by a porous glass diaphragm. A saturated calomel electrode located in a Luggin capillary served as the reference electrode. All potentials are referred to this electrode. An inert nitrogen atmosphere was maintained over the electrolyte. A PAR 273A potentiostat was used to run the experiments. Electrochemical techniques such as linear and cyclic voltammetry and chronoamperometry were used to characterize the catalysts. The electrode activity for methanol oxidation was measured in 1 M $CH_3OH + 0.5$ M H_2SO_4 solution by cyclic voltammetry at a scan rate of 50 mV s^{-1}, starting at 0 V. Chronoamperometry curves were obtained at different potentials, applying potential pulses from an initial potential of 0 V. Current densities are referred to the active surface area.

The morphology of the catalyst surface and the particle size were analyzed using scanning electronic microscopy (SEM, JEOL 100) and atomic force microscopy (AFM, Nanoscope Digitals Instruments, Santa Barbara, USA). The structure of the electrodes was characterized by X-ray diffraction (XRD) using a Rigaku Dmax III C diffractometer with monochromated CuKα radiation. Bulk composition analysis of Pt–Ru catalysts was performed using an X-ray detector for energy dispersive spectroscopy analysis (SEM-EDX). UV-vis spectrophotometry (Agilent 8453) was applied to evaluate the presence of different Pt and Ru complex species and colloid particles formed. For UV-vis analysis all samples were diluted in a ratio 1:50.

Before the electrochemical deposition of the catalyst took place, the carbon supports were treated by anodic potentiostatic polarization in 0.5 M H_2SO_4 at 2 V for 300 s followed by a linear cathodic potential sweep down to -0.8 V (scan rate 1 mV s^{-1}). The surface oxide group reduction produced during the linear sweep improves the activation of the carbon surface [30, 31]. The electrooxidation treatment in aqueous solution at room temperature also forms carboxylic groups, anhydride, quinone, phenolic and lactone groups [32–34]. The presence of all these surface groups modifies the chemical and physical properties of the carbon, improving wettability, adsorption and cation exchange capacity [30, 35], affecting the surface area and stability of supported catalysts. In addition, these oxygen surface groups act as nucleation centers for the generation of highly dispersed metallic crystallites.

The catalysts were synthesized by electrodeposition at room temperature using a dilute solution of platinum and ruthenium salts (2 mM $H_2PtCl_6 + 2$ mM $RuCl_3$ in 0.5 M H_2SO_4) in combination with a stabilizing agent (0.2 M EG, 0.2 M EtOH and 0.2 M HCOOH). Bidistilled water and analytical grade reagents were used. The pH value measured after stabilizer addition was near 2.

Electrodeposition was carried out potentiostatically at -0.5 V for 15 minutes. After deposition, the electrodes were thoroughly rinsed with bidistilled water and tested in sulphuric acid solution. A lineal potential sweep from -0.25 to 0.5 V was applied at a rate of 50 mV s^{-1}. The anodic limit was set to 0.5 V to prevent the formation of inactive ruthenium oxides and to minimize the effect of the electrochemical treatment on the deposit structure.

The active surface area of the electrocatalysts was determined by copper underpotential deposition (Cu-UPD) [36]. Experimental details were described in a previous paper [37].

3 Results and discussion

Figure 1 shows the UV-vis spectral change when the different stabilizing agents were added. In the case of $H_2PtCl_6 + RuCl_3$ solution without stabilizer, there were two absorbance peaks at $\sim$200 and $\sim$260 nm, characteristic of $PtCl_4^{-2}$ and $PtCl_6^{-2}$, respectively [38–40]. The peak

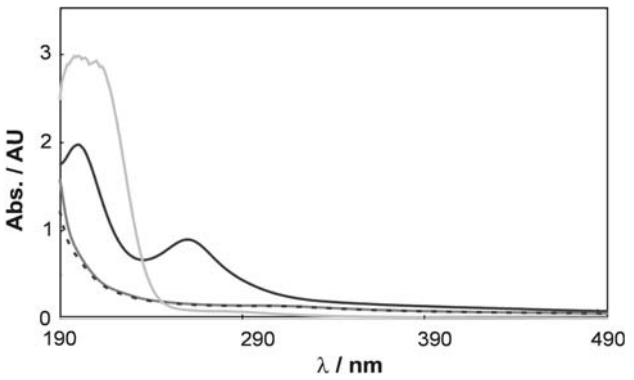

Fig. 1 UV-vis absorption spectra for the solutions containing H_2PtCl_6 and $RuCl_3$, at room temperature. Without stabilizer (▬), EG (▬), EtOH (▬ ▬), and HCOOH (▬)

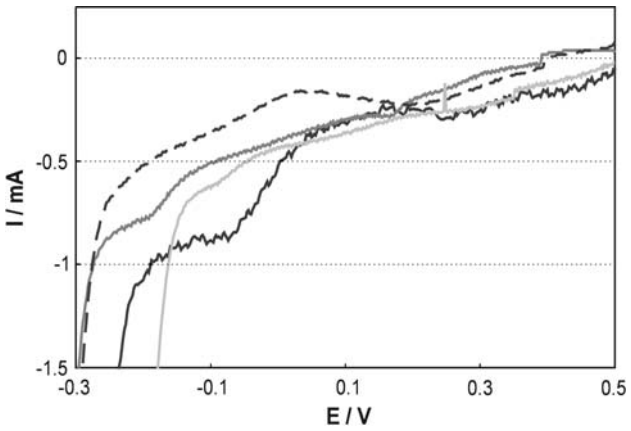

Fig. 2 Voltammetric curves for a GC-10 support in 2 mM H_2PtCl_6 + 2 mM $RuCl_3$ and 0,5 M H_2SO_4. Without stabilizer (▬), EG (▬), EtOH (▬), and HCOOH (▬ ▬). Sweep rate 0.5 mV s^{-1}

at 260 nm is the result of the ligand-to-metal charge transfer transition in the $PtCl_6^{-2}$ ions [40]. However, the characteristic Ru^{+3} ions or the ruthenium hydroxide complexes absorption at 436 nm [41] was absent or masked by the H_2PtCl_6 absorption at this wavelength. The two characteristic absorbance bands disappeared upon the addition of EG and EtOH stabilizing agent. These features confirm the formation of Pt–Ru colloids [42, 43].

When formic acid was added to the solution the absorbance peak at 260 disappeared, but a very wide and strong absorbance peak was seen at 205 nm. In fact this wide peak seems to be the combination of two peaks, one of them centered at 200 nm and the other at 212 nm. According to the literature [44–46], the first one may be attributed to $PtCl_4^{-2}$ formed by reduction of $PtCl_6^{-2}$, whereas the second may be ascribed to the absorbance of colloidal platinum.

Figure 2 shows linear sweep voltammetry curves for Pt and Ru electrodeposition in H_2SO_4 solution containing H_2PtCl_6 + $RuCl_3$ with and without the stabilizing agents respectively. In all the solutions platinum deposition begins at about 0.3 V and the current due to the reaction increases when the potential shifts to more negative values, becoming a mass controlled process at about 0 V. Proton reduction begins near −0.25 V and, at lower potential, occurs simultaneously with platinum reduction. Ruthenium deposition begins at a more negative potential, near 0 V, favoured kinetically by Pt electrodeposition [37].

When the three stabilizers were added to the electrodeposition solution a reduction in the current deposition was observed, which may represent inhibition of the deposition process. The decrease in current can be related to specific adsorption of the stabilizer molecules over the metallic particles thus hindering electrodeposition [47]. Furthermore, when the stabilizing agents are added to the solution a reduction in Pt and Ru ion concentration is produced. The reducing property of EG, EtOH and HCOOH produces colloidal nanoparticles of Pt and Ru, which may give rise to a decrease in the deposition current. During the application of an electric field the electrophoretic deposition (EPD) of the colloidal nanoparticles occurs in a two-step process: a migration process towards the electrode surface and a deposition step proceeding via a complex superposition of electrochemical and aggregation phenomena [48, 49]. The migration step depends on the bulk particle concentration, size distribution, bath conductivity, viscosity and surface charge density [50]. This process can not be observed in the voltammetric curves, because it is a non faradaic process.

Nevertheless, it is not clear, at the moment, which is the predominant mechanism, electrodeposition or electrophoretic deposition, and this will be the object of further work.

The atomic compositions of Pt–Ru/GC-10 electrodes were determined by SEM-EDX. Ru contents near 20 at. % were measured in the electrodes prepared without stabilizer, EG and EtOH, whereas 35 at. % was determined in that prepared with HCOOH. The EDX spectra for the bimetallic catalyst did not show the presence of oxygen in the deposit.

SEM micrographs of Pt–Ru catalysts over graphite clothes are shown in Fig. 3. The electrodeposition method generates rough islands with incipient dendrites. The dendritic shape of the islands is probably a consequence of the interaction between primary and the secondary nucleation, where the depletion zones formed around the metallic nuclei at high overpotential favours secondary nuclei growth, resulting in the formation of ramified structures [51].

The mean particle sizes determined by SEM are presented in Table 1. The addition of a stabilizer has a great effect on particle size. The mean particle size decreases three or four times when EG, EtOH and HCOOH are used as stabilizers and the particle size distribution is relatively narrow. The average size of the particle measured by XRD

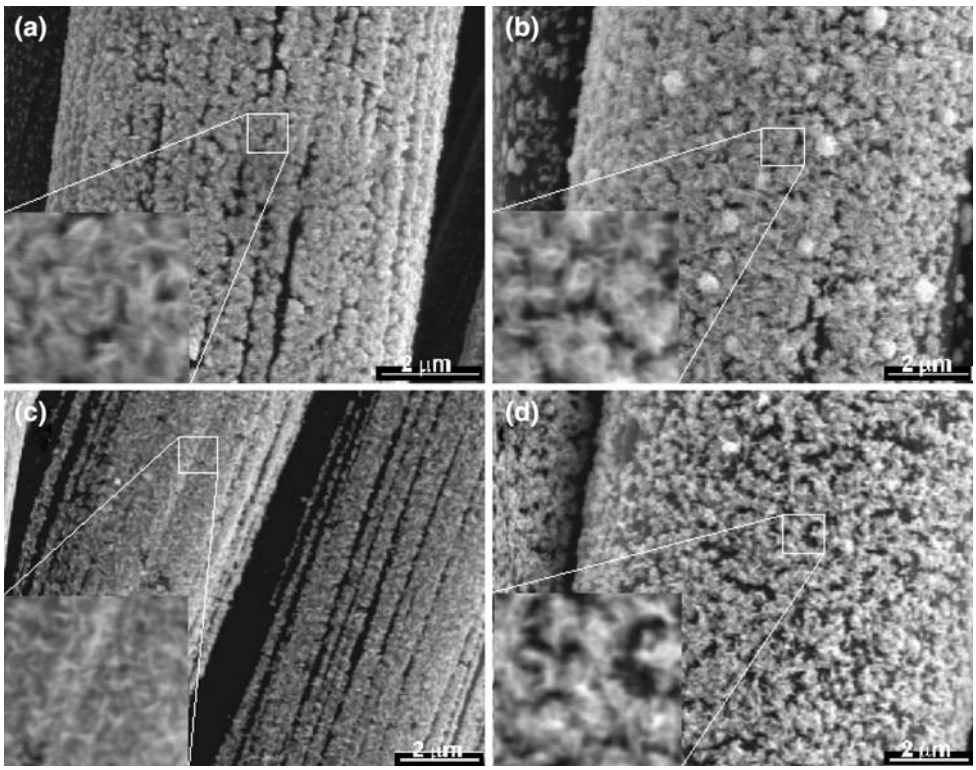

Fig. 3 Top-view SEM images of Pt–Ru/GC-10 electrodes comparing the particles obtained using different stabilizing agents. Without stabilizer (**a**), EG (**b**), EtOH (**c**), HCOOH (**d**). A magnified detail is shown in the left inferior angle of each figure. Pt–Ru catalysts prepared by potentiostatic deposition at −0.5 V for 15 min

Table 1 Mean particle size and active surface area of Pt–Ru catalysts

Pt–Ru catalysts	$d^{a}_{(SEM)}$/nm	$d^{b}_{(AFM)}$/nm	$d^{a}_{(XRD)}$/nm	A^{c}
Without stabilizer	100	100–125	30	61.81
EG	25	25	6	71.33
EtOH	25	25–50	7	92.76
HCOOH	50	50	7	141.36

[a] GC-10 support

[b] GC support

[d] A represent the active surface area per unit of geometric area

spectra is around 5–8 nm, when the catalyst is prepared using the stabilizing agents, whereas, the mean particle size is near 30 nm when there is no stabilizer. This means that the Pt–Ru particles determined by SEM microscopy are in, fact, agglomerates comprising much smaller particles. Diffraction peaks for Ru were not observed in the XRD spectra. This indicates that Ru is at least partially dissolved in the Pt fcc lattice forming an alloy. Furthermore, the presence of platinum and ruthenium oxides was not observed in the analysed samples. Some structural differences of the deposits obtained with the different baths were revealed by X-ray diffractograms. Typical peaks of the crystalline face centred cubic Pt [111], [101], [100], [200] and [220] planes were clearly visible. However, some of the planes were absent in the different electrodes, particularly the plane [200] in the electrode prepared without stabilizer, the plane [100] in the electrodes preparing with EG, EtOH and HCOOH, and the plane [220] in EG and HCOOH electrodes.

The preferred orientation, given by the ratio of reflection intensities, was the crystallographic direction [111] for the electrodes prepared using EG, EtOH and without stabilizer, whereas that corresponding with the plane [101] was predominant for the electrode prepared using HCOOH]. In addition, for the electrode prepared without stabilizer the diffraction peak corresponding to the plane [220] was the second preferred orientation, whereas for the electrodes prepared using EtOH and HCOOH it was the plane [200], and the plane [101] for the electrodes prepared using EG.

Pt–Ru electrodes were also prepared using GC as support. The Pt–Ru electrodeposits were studied by AFM microscopy (Fig. 4). The AFM images showed metallic agglomerates comprising smaller particles. All the electrodes presented a very rough surface. The catalyst particles were homogenously distributed over the support surface as observed in GC-10 electrodes, but the particle shape was very different from that observed in SEM images. This difference may be associated with the effect produced by the AFM tip in the observed images. The mean particle size determined by AFM can be seen in Table 1. The values agree with those determined from SEM images.

A large effect in the active surface area per unit of geometric area, A, is obtained when the stabilizers are added to the solution (Table 1). The largest active surface area is obtained with HCOOH, followed by EtOH and EG.

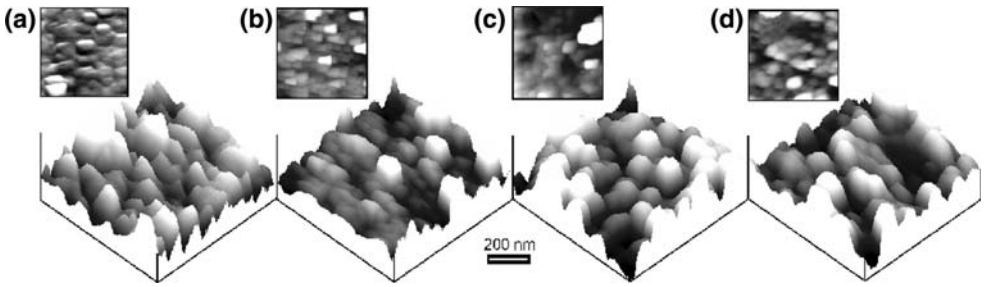

Fig. 4 Top-view and 3D AFM images of Pt–Ru/GC electrodes. Without stabilizer (**a**), EG (**b**), EtOH (**c**), HCOOH (**d**). Pt–Ru catalysts prepared by potentiostatic deposition at −0.5 V for 15 min

This can be related to a reduction in the particle size and a more homogeneous distribution of the metallic particles over the carbon support when stabilizers are added. The different behaviour of the stabilizing agents may be associated with four different effects: (1) the capability of the stabilizing agent to complex the metal ions, (2) the specific adsorption of organic molecules which inhibits particle growth, (3) the reduction in the polarity of the electrolytes which improves ion exchange of Pt and Ru ions with the oxygen groups formed over the support surface, and (4) the reduction capability of the organic compounds.

The first point is connected to the existence of species such as carboxyl anion groups that can act as a stabilizer forming chelate-type complexes with platinum and ruthenium ions [29]. However this effect should not be so important because the solution is very acidic and the quantity of carboxyl anion groups is much reduced.

The reversible specific adsorption of the molecules on the electrode surface hinders surface diffusion of the adatoms. The free electron pairs of the oxygen atoms in organic molecules interact strongly with Pt–Ru particles and therefore the inhibiting effect is very strong, as observed for the systems nano-copper/citric acid [18], nano-nickel/saccharin [52], and nano-silver/EDTA [53].

The addition of EG, EtOH and HCOOH with relative permitivities of 37.8, 24, and 58.3 respectively, only has a small impact on the ionic conductivity of the deposition electrolyte [54], but this effect may be sufficiently important to reduce the particle size.

Figure 5 shows the cyclic voltammograms recorded at 50 mV s^{-1} in 1 M CH_3OH + 0.5 M H_2SO_4 at room temperature. The results of methanol electrooxidation for the electrodes prepared under the different conditions are summarized in Table 2. For all the electrodes the onset of the methanol oxidation reaction takes place near 0.2 V. The beginning of methanol oxidation at this potential is associated with the formation of OH_{ads} species on Ru atoms originating in the water dissociation that occurs at potentials more negative than that on Pt atoms, through the so called bifunctional mechanism [55, 56].

The voltammograms suggests that PtRu/GC-10 catalyst prepared using EtOH as stabilizer has the greatest activity for methanol oxidation, followed by the electrode prepared

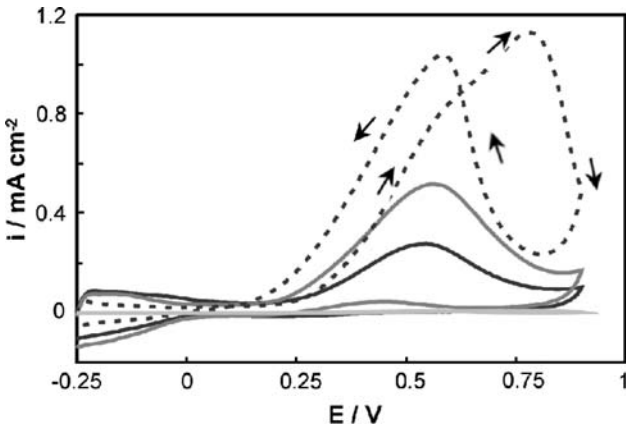

Fig. 5 Cyclic voltammograms for Pt–Ru/GC-10 electrodes in 1 M CH_3OH/0.5 M H_2SO_4, at room temperature. Without stabilizer (▬), EG (▬), EtOH (▬ ▬), and HCOOH (▬). Scan rate 50 mV s^{-1}. Pt–Ru catalysts prepared by potentiostatic deposition at −0.5 V for 15 min

Table 2 Electrocatalytic properties of Pt–Ru catalysts

Electrode Pt–Ru/GC-10	I_p (mA)	i_p (mA cm^{-2})	E_p (V)
Without stabilizer	17.0	0.28	0.55
EG	37.0	0.52	0.56
EtOH	104.3	1.12	0.65
HCOOH	53.0	0.037	0.57

Data from cyclic voltammograms

using EG. However, the electrode prepared using HCOOH has less activity for methanol oxidation than that prepared without stabilizer. Both the catalyst activity to methanol oxidation and the active surface area increase when the particle size decreases. Nevertheless, this good correlation is not fulfilled for the electrode prepared using HCOOH. To compare the activity of different catalysts for methanol oxidation it is necessary to take into the account both particle size and active surface area, and not only one of them. However, the differences in the intrinsic activity of the electrodes prepared with different stabilizing agents cannot be explained as a function of particle size and active surface area. Probably, these differences may be due to changes in the superficial composition or to differences in the crystalline structure of the deposits. The anomalous

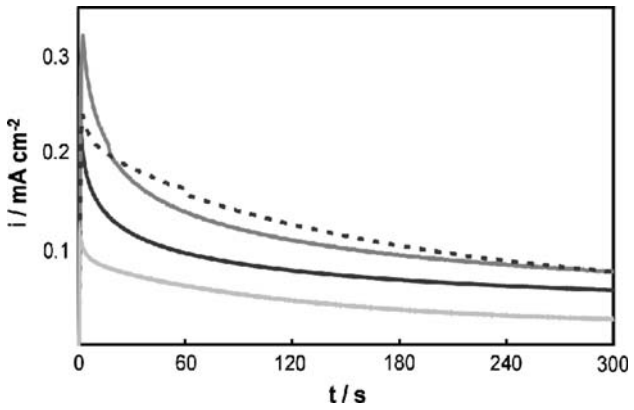

Fig. 6 Chronoamperometry curves at 0.4 V for Pt–Ru/GC-10 electrodes in 1 M CH_3OH/0.5 M H_2SO_4, at room temperature. Without stabilizer (▬), EG (▬), EtOH (▬ ▬), and HCOOH (▬). Pt–Ru catalysts prepared by potentiostatic deposition at −0.5 V for 15 min

Table 3 Electrocatalytic performance of the Pt–Ru catalysts

Electrode Pt–Ru/GC-10	0.2 V	0.3 V	0.4 V	0.5 V
		i (mA cm^{-2})		
Without stabilizer	0.0005	0.0272	0.0639	0.0743
EG	0.0002	0.0324	0.0875	0.1005
EtOH	0.0003	0.0134	0.0942	0.2145
HCOOH	0.0007	0.0050	0.0328	0.0648

Data from chronoamperometry curves after 300 s

behaviour observed with the Pt–Ru catalyst prepared with HCOOH as stabilizer was a consequence of the higher Ru content in the electrode. It is known that a Pt–Ru alloy with low Ru content (10–20 at. %) exhibits the best performance for methanol oxidation at room temperature [57]. Higher Ru content reduces the available surface sites where the methanol adsorption reaction is taking place, reducing the activity of the catalyst. This result can be easily explained using the statistical interpretation of bifunctional Pt–Ru electrodes suggested by Gasteiger et al. [57].

Current transient measurements at constant potentials were carried out for 300 s (Fig. 6), showing that the different electrodes present the same behaviour as that observed in the voltammograms. The results are summarized in Table 3.

4 Conclusions

The following conclusions can be drawn: (1) the electrochemical activation of the electrodes studied generates surface oxygenated groups that increase the hydrophilic character of the surface and act as attachment centers for metallic particles; (2) the use of stabilizing agents produces a decrease in size of Pt–Ru nanoparticles, and an increase in the catalyst active surface area, following the order HCOOH > EtOH > EG > no stabilizing agent; (3) the activity for methanol oxidation increases when EtOH and EG are used as stabilizer and (4) to evaluate the catalytic activity of an electrode it is necessary to take into account the interaction between particle size and active surface area.

Acknowledgements This work was supported by ANPCYT Grant No. 10-11133l, CIC and SECyT UNS, Argentina. J.M. Sieben acknowledges CONICET for a doctoral fellowship. The assistance by M.E. Brigante in the UV-vis measurements is also acknowledged.

References

1. Rao CRK, Trivedi DC (2005) Coord Chem Rev 249:613
2. Coutanceau C, Rakotondrainibe AF et al (2004) J Appl Electrochem 34:61
3. Wei ZD, Chan SH (2004) J Electroanal Chem 569:23
4. Wei ZD, Chan SH et al (2005) Electrochim Acta 50:2279
5. Shen M, Roy S, Scott K (2005) J Appl Electrochem 35:1103
6. Hogarth MP, Punk J et al (1994) J Appl Electrochem 24:85
7. Duarte MME, Pilla AS et al (2006) Electrochem Commun 8:159
8. Maillard F, Gloaguen F, Léger JM (2003) J Appl Electrochem 33:1
9. Aramata A, Kodera T, Masuda M (1988) J Appl Electrochem 18:577
10. Niu L, Li Q et al (2005) J Electroanal Chem 578:331
11. Lee CH, Lee CW et al (2002) Int J Hydrogen Energy 27:445
12. Tusseeva EK, Mikhaylova AA et al (2004) Russian J Electrochem 40:1146
13. Chrzanowski W, Wieckowski A (1997) Langmuir 13:5974
14. Vigier F, Gloaguen F et al (2001) Electrochim Acta 46:4331
15. Iúdice de Souza JP, Iwasita T et al (2000) J Appl Electrochem 30:43
16. Rodríguez-Nieto FJ, Morante-Catacora TY, Cabrera CR (2004) J Electroanal Chem 571:15
17. Selvaraju T, Ramaraj R (2005) J Electroanal Chem 585:290
18. Natter H, Hempelmann R (1996) J Phys Chem 100:19525
19. Alfantazi AM, Erb U (1996) J Mater Sci Lett 15:1361
20. Dalmia A, Lineken CL, Savinell RF (1998) J Colloid Interface Sci 205:535
21. Obradović MD, Stevanović RM, Despić AR (2003) J Electroanal Chem 552:185
22. Younes O, Zhu L et al (2001) Langmuir 17:8270
23. Guaus E, Torrent-Burgués J (2005) J Electroanal Chem 575:301
24. Zarkadas GM, Stergiou A, Papanastasiou G (2001) J Appl Electrochem 34:1251
25. Zarkadas GM, Stergiou A, Papanastasiou G (2005) Electrochim Acta 50:5022
26. Mu Y, Liang H et al (2005) J Phys Chem B 109:22212
27. Lordi V, Yao N, Wei J (2001) Chem Mater 13:733
28. Matsumoto T, Komatsu T et al (2004) Catal Today 90:277
29. Bock C, Paquet C et al (2004) J Am Chem Soc 126:8028
30. Duarte MME, Pilla AS et al (1993) An Asoc Quím Argent 81:415
31. Duarte MME, Mayer CE (1997) An Asoc Quím Argent 85:27
32. Randin JP (1976) In: Bard J (ed) Encyclopedia of Electrochemistry of the Elements, vol 7. Marcel Dekker, New York, p 22
33. Olender H, O'Grady WE et al (1982) J Appl Electrochem 12:135
34. Jovanović DM, Terzić S et al (2004) Electrochem Commun 6:1254

35. Antonucci PL, Alderucci V et al (1994) J Appl Electrochem 24:58
36. Green CL, Kucernak A (2002) J Phys Chem B 106:1036
37. Sieben JM, Duarte MME, Mayer CE (2008) J Appl Electrochem 38:483
38. Ravadullar JF, Vergara MC et al (1997) J Phys Chem B 101:8997
39. Henglein A, Ershov BG, Malow M (1995) J Phys Chem 99:14129
40. Teranashi T, Hosoe M et al (1999) J Phys Chem B 103:3818
41. Pârvulescu VI, Coman S et al (1999) Appl Surf Sci 141:164
42. Duff DG, Edwards PP, Johnson BFG (1995) J Phys Chem 99:15934
43. Chen S, Kimura K (2001) J Phys Chem B 105:5397
44. Chen ChW, Takezako T et al (2000) Colloids Surf A 169:107
45. Creighton A, Eadon DG (1991) J Chem Soc Faraday Trans 87:3881
46. Zhou Z, Zhou W et al (2004) Catal Today 93–95:523
47. Wang H, Zhao Y et al (2006) J Power Sources 155:33
48. Israelachvili N (1992) Intermolecular and surface forces, 2nd edn. Academic Press, New York, p 248
49. Bouyer F, Foissy A (1999) J Am Ceram Soc 82:2001
50. Besra L, Liu M (2007) Progress Mater Sci 52:1
51. Plyasova LM, IYu Molina et al (2006) Electrochim Acta 51:4477
52. Natter H, Schmelzer M, Hempelmann R (1998) J Mater Res 13:1186
53. de Oliveira GM, Barbosa LL et al (2005) J Electroanal Chem 578:151
54. Tsai MCh, Yeh TK, Tsai ChH (2006) Electrochem Commun 8:1445
55. Watanabe M, Motoo S (1976) J Electroanal Chem 69:429
56. Gasteiger HA, Marković N et al (1994) J Electrochem Soc 141:1795
57. Gasteiger HA, Marcović N et al (1993) J Phys Chem 97:12020